Available online at www.sciencedirect.com

ScienceDirect

Polymer 47 (2006) 6782–6796

polymer

www.elsevier.com/locate/polymer

A model of charge transport and electromechanical transduction in ionic liquid-swollen Nafion membranes

Matthew D. Bennett [a,*], Donald J. Leo [a], Garth L. Wilkes [b], Frederick L. Beyer [c], Todd W. Pechar [b]

[a] Center for Intelligent Material Systems and Structures, Virginia Tech, Department of Mechanical Engineering, 310 Durham Hall, Blacksburg, VA 24061, USA
[b] Polymer Materials and Interfaces Laboratory, Virginia Tech, Department of Chemical Engineering, 133 Randolph Hall, Blacksburg, VA 24061, USA
[c] U.S. Army Research Laboratory, Materials Division, Aberdeen Proving Ground, MD 21005, USA

Received 31 May 2006; accepted 17 July 2006

Abstract

Ionomeric polymer transducers (sometimes called “ionic polymer–metal composites,” or “IPMCs”) are a class of electroactive polymers that are able to operate as distributed electromechanical actuators and sensors. Traditionally, these transducers have been fabricated using water-swollen Nafion membranes. This work seeks to overcome the hydration dependence of these transducers by replacing water with an ionic liquid. In the current work, two ionic liquids are studied as diluents for ionomeric polymer transducers based on Nafion membranes. The two ionic liquids used are 1-ethyl-3-methylimidazolium trifluoromethanesulfonate (EMI-Tf) and 1-ethyl-3-methylimidazolium bis(trifluoromethanesulfonyl)imide (EMI-Im). These two ionic liquids were chosen for their low viscosity and high conductivity. Furthermore, although many of the physical properties of the two ionic liquids are similar, the EMI-Tf ionic liquid is water miscible whereas the EMI-Im ionic liquid is hydrophobic. These important similarities and differences facilitated investigations of the interactions between the ionic liquids and the Nafion polymer.

This paper examines the mechanisms of electromechanical transduction in ionic liquid-swollen transducers based on Nafion polymer membranes. Specifically, the morphology and relevant ion associations within these membranes are investigated by the use of small-angle X-ray scattering (SAXS), Fourier transform infrared (FTIR) spectroscopy, and nuclear magnetic resonance (NMR) spectroscopy. These results reveal that the ionic liquid interacts with the membrane in much the same way that water does, and that the counterions of the Nafion polymer are the primary charge carriers in the ionic liquid-swollen films. The results of these analyses are compared to the macroscopic transduction behavior in order to develop a molecular/morphological model of the charge transport mechanism responsible for electromechanical coupling in these membranes.

Keywords: Electroactive polymer; Charge transport; IPMC

---

1. Introduction

In the late 1940s it was discovered that ion containing polymers could be used as electrochemomechanical transducers. The pioneering work in this field was performed by Kuhn et al. [1,2] of the University of Basle (Switzerland) and Katchalsky et al. [2,3] of the Weizmann Institute of Science (Israel). More recently, several researchers have shown that Nafion ionomer membranes can function as electromechanical transducers [4–6]. DuPont’s Nafion is one of the most common ion-exchange polymers in use today.

Nafion consists of a Teflon-like backbone chain with pendant side chains that are terminated in neutralized sulfonate exchange sites. The chemical structure of Nafion is shown in Fig. 1. In this figure, m is typically 1 and n varies from 5 to 11. The value of n is related to the degree of sulfonation of the polymer, which is reported as the equivalent weight (EW) of the membrane. The equivalent weight is defined as the weight of dry polymer per mole of exchange sites and for Nafion is typically in the range from 900 to 1500. Lower

---

* Corresponding author. Tel.: +1 540 239 4198; fax: +1 540 231 2903.
E-mail address: mabenne2@vt.edu (M.D. Bennett).

0032-3861/$ - see front matter © 2006 Elsevier Ltd. All rights reserved.
doi:10.1016/j.polymer.2006.07.061

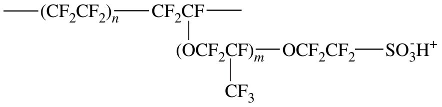

$$-(CF_2CF_2)_n-CF_2CF- \quad | \quad (OCF_2CF)_m-OCF_2CF_2-SO_3^-H^+ \quad | \quad CF_3$$

Fig. 1. The chemical structure of Nafion polymer.

values of EW are equivalent to higher ion content in the polymer. In Fig. 1, the ionomer is shown in its proton form. However, the hydrogen ion can be exchanged for any other cation.

If coated on both sides with a conductive electrode and swollen with a suitable diluent, a Nafion membrane can be made to act as an electromechanical transducer. The membrane bends towards the anode upon application of an electric field. It is believed that this bending is due to the motion of the mobile cations and diluent within the polymer matrix. Mallavarapu and Leo [7] and Kothera and Leo [8] have shown that feedback may be used effectively to control the motion of these actuators in a free bender configuration. Nafion membranes also exhibit the converse behavior of sensing mechanical deformation. It is believed that macroscopic motion of the membrane produces microscopic motion of the mobile cations, resulting in a charge imbalance across the electrodes. Several researchers have demonstrated that the quasi-static displacement of the polymer is correlated with the voltage that is produced by the membrane [6,9,10]. More recently, Newbury and Leo demonstrated that the current induced in the membrane is proportional to the rate of the mechanical deformation [11,12].

One of the obstacles to widespread use of ionomeric polymer transducers is their hydration dependence. In order for the transduction to occur, the cations must be mobilized by swelling the polymer with a diluent, which has typically been water. The use of water as a diluent has limited the commercial applications of these transducers. One possible solution to this problem is to utilize a barrier coating to contain the water within the membrane. Bar-Cohen et al. reported that a transducer coated with a barrier layer was able to operate in air for four months [13,14]. However, such a barrier coating will add passive stiffness to the actuator device and reduce the amount of strain that the device can generate [15]. Also, the small electrochemical stability window of water limits the maximum operating voltage and the amount of strain and stress that the actuators can generate.

The goal of this work is to replace water with an ionic liquid. Ionic liquids are a class of unique solvents that contain only charged species and have many interesting properties that make them attractive for application in ionomeric polymer transducers. The vapor pressure of ionic liquids is immeasurably low, so they will not evaporate out of the ionomeric polymer transducer when it is operated in air. Bennett and Leo have previously demonstrated transduction in ionic liquid-swollen Nafion membranes [16]. They showed that an ionic liquid-swollen transducer could be operated for over 250,000 cycles in air with less than 30% decrease in the free strain generated. In contrast, a water-swollen transducer stopped working after only 3000 cycles under the same conditions. Among others, Lu et al. [17], Ding et al. [18], and Vidal et al. [19] have also shown that ionic liquids may be used as electrolytes for conducting polymer actuators. By replacing the traditional organic and aqueous electrolytes with ionic liquids, these authors demonstrated stable operation of conducting polymer actuators in air. In addition to their low volatility, ionic liquids are also inherently very thermally stable. Therefore, ionic liquid-swollen transducers can withstand high temperature processing that would not be possible with their water-swollen counterparts. Ionic liquids also have a larger electrochemical stability window than water, meaning that the transducers can be operated at higher voltages.

The focus of this research is the development of a model of the transduction mechanisms in ionic liquid-swollen Nafion membranes. This model is based on observations of the morphology of the membranes by small-angle X-ray scattering (SAXS), observations of the ion associations by Fourier transform infrared (FTIR) spectroscopy and nuclear magnetic resonance (NMR) spectroscopy, and observations of the electromechanical transduction behavior. The results of these studies are combined to explain the interactions of the ionic liquid with the ionomer and the role of the ionic liquid in transduction.

2. Sample preparation

Previous investigations into the use of ionic liquids as diluents for ionomer membrane transducers have been performed by Bennett and Leo [16,20]. Based on the results of these initial studies, the ionic liquids 1-ethyl-3-methylimidazolium trifluoromethanesulfonate and 1-ethyl-3-methylimidazolium bis(trifluoromethanesulfonyl)imide were chosen for this work. These will be abbreviated as "EMI-Tf" and "EMI-Im," respectively. These ionic liquids were chosen primarily for their low viscosity and high conductivity. The structures of these ionic liquids are shown in Fig. 2 and the properties are presented in Table 1. As can be seen, the properties of the ionic liquids are relatively similar except for their hydrophobicity and viscosity. Whereas the EMI-Tf ionic liquid is water miscible, the EMI-Im ionic liquid is hydrophobic. Also, the EMI-Im ionic liquid is slightly less viscous than the EMI-Tf ionic liquid. The anion of the EMI-Im ionic liquid is also larger than the anion of the EMI-Tf ionic liquid, and more

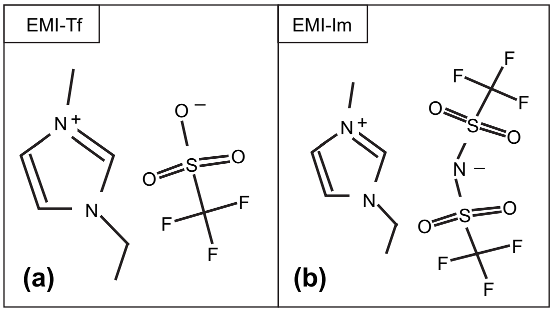

Fig. 2. Chemical structure of (a) 1-ethyl-3-methylimidazolium trifluoromethanesulfonate ionic liquid, and (b) 1-ethyl-3-methylimidazolium bis(trifluoromethanesulfonyl)imide ionic liquid.

Table 1
Properties of the two ionic liquids

Ionic liquid	Viscosity (cP at 25 °C)	Density (g/cm^3)	Melting point (°C)	Conductivity (mS/cm at 25 °C)	Sat. water content (mass% at 20 °C)	Electrochemical stability window (V)
EMI-Tf	45 [21]	1.390 [21]	−9 [21]	8.6 [21]	Soluble [21]	4.1 [21]
	43 [22]	1.383 [22]	−10 [22]	9.3 [22]		
EMI-Im	34 [21]	1.520 [21]	−3 [21]	8.8 [21]	1.4 [21]	4.3 [21]

highly fluorinated. This contributes to the higher molecular weight of the EMI-Im ionic liquid (331.25 g/mol for EMI-Im as compared to 260.23 g/mol for EMI-Tf) and is also likely related to its more hydrophobic character.

The experimental parameters that were varied in the current study were the counterion of the Nafion membrane, the structure of the ionic liquid, and the content of the ionic liquid within the membrane. Nafion-117 membranes (EW 1100, nominal thickness 183 μm) in the protonated form were utilized and were pretreated by boiling in 1.0 M sulfuric acid followed by boiling in DI water. The membranes were then exchanged from the proton form to one of the six neutralized forms by soaking in 0.5 M aqueous chloride salt solutions. The six cation forms of the membrane studied were lithium, sodium, potassium, cesium, 1-ethyl-3-methylimidazolium (EMI), and tetraethylammonium (TEA). After soaking in the chloride salt solutions for several days, the membranes were thoroughly rinsed and soaked in DI water for 3 h to remove any excess salt. They were then dried overnight at 110 °C under vacuum. The dry weight of the membranes was recorded and they were then swollen with ionic liquid.

Following the pretreatment described above, the membranes were swollen with one of the two ionic liquids. In order to facilitate the incorporation of the ionic liquids by the Nafion membranes, they were mixed with methanol and different combinations of time and temperature were used for the soak. For the samples that were tested by FTIR and NMR, the pretreated and dried membranes were swollen by soaking in a mixture of two parts ionic liquid (by volume) to one part methanol. Five different uptakes were targeted and the amount of time that the dry membranes were allowed to soak in the ionic liquid/methanol mixture was varied from less than 1 min to over 2 h at room temperature. For the highest uptake, the membranes were soaked for 2.5 h at 65 °C. Following the swelling of the membranes with ionic liquid, they were dried under vacuum at 110 °C for 3 h to remove the methanol. For the samples that were tested by SAXS, the dry membranes were swollen with ionic liquid by soaking in a mixture of one part ionic liquid (by volume) and one part methanol for 3 h at either 25 °C, 70 °C, or 90 °C. After this soak the membranes were dried under vacuum at 110 °C for 3 h. By holding the membranes at an elevated temperature following the ionic liquid incorporation step, uniform dispersion of the ionic liquid within the membranes is ensured. This is especially important for those membranes where the uptake of ionic liquid is very low.

The loading of ionic liquid within the Nafion membranes was determined from the weight gain during the swelling process. In this paper, the uptake of ionic liquid will be reported in two forms: as a volumetric percentage normalized by the dry volume of the membrane, and as a molar ratio relative to the number of sulfonate exchange sites in the membrane. The volumetric uptake of ionic liquid was determined from

$$V = 100\left(\frac{(w_s - w)\rho}{w\rho_i}\right) \tag{1}$$

where w_s is the swollen weight of the membrane, w is the dry weight of the membrane, ρ is the density of the dry membrane, and ρ_i is the density of the ionic liquid. The dry density of the membranes was determined from weight and volume measurements of dried samples. A minimum of four density measurements was averaged for each data point. The ratio of number of moles of ionic liquid to moles of exchange sites was determined from

$$f = (w_s - w)\left(\frac{1100}{wM_i}\right) \tag{2}$$

In this equation, 1100 is the equivalent weight of the Nafion-117 membrane, in grams of dry polymer per mole of exchange sites, w_s is the weight of the swollen film, w is the weight of the dry film, and M_i is the molecular weight of the ionic liquid (260.23 g/mol for EMI-Tf and 331.25 g/mol for EMI-Im).

For the samples that were tested by SAXS, FTIR, and NMR, no electrodes were deposited onto the membranes. However, for the membranes that were investigated as electromechanical transducers, electrodes were deposited onto each surface of the films using one of two methods. Several researchers have shown that the actuation mechanism in ionomeric polymer transducers is related to the formation of a charge imbalance across the thickness of the film [23–25]. Akle et al. have related the free strain generated by an ionomeric transducer to the capacitance of the device [26]. Therefore, a critical feature of the electrodes is the interfacial area between the ionomer and the metal. As this area is increased, the charge capacity of the membrane is increased, thus increasing the strain generation potential. A common method for fabricating high surface area electrodes for ionomeric transducers involves the electroless reduction of platinum on the surfaces of a Nafion membrane [27–29].

In this work the platinum plating process was carried out as follows. A Nafion-117 membrane was first sanded on both sides in a 90° cross-hatching pattern using 600-grit sandpaper. The membrane was then pretreated by boiling in 1.0 M sulfuric acid and DI water. The plating process was begun by soaking the membrane in an aqueous solution of tetraammineplatinum chloride ($Pt(NH_3)_4Cl_2$). The membrane was then removed from the solution, rinsed thoroughly with DI water, and soaked in an aqueous solution of 0.1% (by weight) sodium borohydride ($NaBH_4$) for 8 h, without stirring or agitation. The sodium borohydride reduced the absorbed $Pt(NH_3)_4^{2+}$ ions in the membrane to metallic platinum, at the surface of the membrane and also within the polymer, to a depth of about 10–20 μm. The platinum electrode forms within the membrane as a uniformly dispersed layer of particles whose concentration decreases with increasing penetration depth. Following the reduction process, the membrane was boiled in 1.0 M H_2SO_4 for 1 h to exchange it back into the proton form. In order to increase the loading of platinum metal within the surfaces of the membrane, the plating process was repeated a total of five times. After the platinum plating process, the membrane was again boiled in 1.0 M H_2SO_4 and was then cut into several pieces. Each piece was then soaked for several days in a 0.5 M aqueous chloride salt solution to convert it into a desired cation form. The membranes were then thoroughly rinsed with DI water and dried at 110 °C under vacuum for 12 h before being swollen with ionic liquid.

Electromechanical characterizations were also performed on membranes that were plated using a newer "direct assembly" process developed by Akle et al. [30]. In this process, a mixture was prepared containing 87.4% (by weight) of a commercially available Nafion dispersion (5% Nafion by weight) and 12.6% (by weight) of ruthenium dioxide (RuO_2) powder. The RuO_2 particles were dispersed by stirring and sonication. This solution was then sprayed onto two fiberglass-reinforced Teflon decals in many layers using an airbrush, with each layer dried by heating under a lamp. The electrodes were then transferred to a sodium-form Nafion membrane by hot-pressing at 210 °C under a pressure of 14 MPa for 8 min. Following the hot-pressing, the decals were peeled away. With the RuO_2 electrodes in place, the membranes were boiled in 1.0 M H_2SO_4 and in DI water and were then cut into several pieces. Each piece was soaked in 0.5 M aqueous chloride salt solutions in order to exchange the cation within the membrane. For both of the plating processes that were used in this work, the electrodes were applied to a large piece of Nafion that was then cut into smaller pieces. This approach helped to ensure that the electrodes were uniform and consistent on each sample that was tested. After the smaller pieces were exchanged into the appropriate cation form, they were dried at 110 °C under vacuum for 12 h and swollen with ionic liquid.

The membranes tested as electromechanical transducers were swollen with ionic liquid using the methods described previously. The uptake of ionic liquid within the membranes was determined by measuring the weight gain of the membrane during the swelling process and was calculated using Eqs. (1) and (2). However, for the transducer samples, the density of the dry membranes was measured after the interpenetrating (platinum or RuO_2) electrode had been deposited. This allowed for the additional weight of the electrode to be accounted for in the determination of the uptake of ionic liquid. For the transducer samples plated with RuO_2 electrodes, the swelling was carried out by soaking in a mixture of two parts ionic liquid (by volume) to one part methanol for a predetermined amount of time at room temperature. For the highest uptake, the membranes were soaked for 2.5 h at 65 °C. For the platinum-plated transducers, the dry membranes were swollen with ionic liquid by soaking in a mixture of one part ionic liquid (by volume) and one part methanol for 3 h at either 25 °C, 70 °C, or 90 °C. After this soaking of the transducers in the ionic liquid/methanol mixture, the membranes were dried under vacuum at 110 °C for 3 h to remove the methanol.

The interpenetrating platinum and ruthenium dioxide electrodes deposited using the procedures described possess a large interfacial area with the Nafion polymer, an important consideration for ionomeric transducers. However, the electrodes do not possess a high electrical conductivity along the length of the transducer strips, resulting in large Ohmic losses and a decrease in the performance of the devices. In order to overcome this problem, a second surface electrode was applied on top of the interpenetrating metal layers. In previous works this electrode was often applied by electroplating of gold directly onto the platinum layer. However, Bennett and Leo have noted that when the gold plated transducers were dried and then swollen with ionic liquid, cracking of this layer often results, dramatically decreasing the conductivity of the surface electrodes [20]. For this reason, a new process has been developed in which the gold layer is applied *after* the membranes have been swollen with ionic liquid. This gold electrode is made up of two parts: a binder layer and a thin gold foil. In the case of the platinum-plated samples, the binder layer consisted of Nafion polymer that was applied by painting from a 5% dispersion (by weight). In the case of the RuO_2-plated membranes, a linear poly(urethane urea) was used as the binder layer and was applied by painting from a 3% (by weight) solution in a mixed solvent of 50% (by weight) isopropyl alcohol and 50% tetrahydrofuran. The synthesis and properties of the poly(urethane urea) have been reported previously [31]. After drying the binder layer, the membranes were sandwiched between two waxed paper-backed gold leaves (approximately 50–100 nm in thickness) and pressed at 170 °C and 2.5 MPa for 10 s. The waxed paper was then peeled away and the edges of the samples were trimmed prior to testing.

3. Experimental methods

3.1. Small-angle X-ray scattering

The ionic liquid-swollen Nafion membranes have been characterized using a number of analytical techniques and equipment. Small-angle X-ray scattering was performed on a pinhole-collimated system at the Army Research Lab using X-rays with a wavelength of 1.542 Å. Ionic liquid-swollen strips of Nafion-117 membrane approximately 1 × 5 cm and 0.2 mm in thickness were attached to a sample holder using double-sided tape. In order to obtain a sufficient number of scattered X-ray strikes on the multiwire detector, each sample was illuminated for 40 min. To convert this image into a curve of scattered intensity versus the length of the scattering vector, the two-dimensional scattering pattern was azimuthally averaged. The data were then corrected for detector noise and background scatter, and then scaled to absolute intensity using a glassy carbon calibrant. The radial positions of the scattered X-rays were then used to determine the lattice spacing, where the lattice spacing, d, is related to the length of the scattering vector, q, by $q = 2\pi/d$.

3.2. Fourier transform infrared spectroscopy

These membranes were also tested using Fourier transform infrared spectroscopy. For this testing, ionic liquid-swollen films approximately 1 × 5 cm were pressed against a thallium bromoiodide crystal (KRS-5) with 45° beveled ends using a thumbscrew pressure plate assembly. Prior to the testing of the films, a scan of the background emissivity of the ATR system was performed. This emissivity was used as a baseline against which the absorbance of each sample was measured. The sample chamber was continuously purged with dry air during the testing in order to reduce the effect of moisture on the results. The chamber was allowed to purge undisturbed for 30 min prior to the measurement of the background emissivity and approximately 5 min between the testing of each sample. A total of 64 scans of each sample were averaged in order to increase the signal-to-noise ratio of the data and the broadband absorbance of the samples was converted into 3733 distinct spectral lines using a Fourier transform. This yielded clean spectra for the ionic liquid-swollen films over a range of wavenumbers from 400 cm^{-1} to 4000 cm^{-1}. This technique was also used to measure the absorbance spectra of the neat ionic liquids by spreading a small drop of ionic liquid over the surface of the crystal. The crystal was carefully cleaned when necessary using methyl-ethyl ketone (MEK).

3.3. Nuclear magnetic resonance spectroscopy

Alkali metal NMR was also performed on samples of ionic liquid-swollen Nafion membranes in the sodium, lithium, and cesium counterion forms. In order to perform this testing, Nafion films 5 × 10 cm were pretreated and swollen with ionic liquid as described in Section 2. The samples were then cut into strips 0.5 × 5 cm, which were stacked and inserted into a 10 mm NMR tube. For the lithium- and cesium-form membranes, glass tubes were used. For the sodium-form membranes, Teflon tubes were used to prevent interference from the sodium present in the glass. In all cases, the tubes were back-filled with dry nitrogen gas and tightly sealed to prevent absorption of humidity by the films. NMR spectra were obtained using a standard 90° pulse on a Varian Unity 400 spectrometer in the NMR lab at Virginia Tech. A total of 200–500 scans were recorded for each sample in order to increase the signal-to-noise ratio of the data. The field strength of the spectrometer was 9.39 T and the relevant parameters of the testing used for each isotope are listed in Table 2. The acquisition time is the length of time during which data is recorded after each pulse. The relaxation delay is a dwell after the completion of data collection and prior to the start of the next pulse. The program NUTS (Acorn NMR Inc.) was used to process the raw data from the spectrometer. After transforming the free induction decay to the frequency domain, the peak width was determined at half of the peak height. Additionally, a line broadening technique was used to increase the signal-to-noise ratio of the data. In order to correct for this, the additional width introduced by the line broadening was subtracted from the measured peak width.

Table 2
Parameters used for the NMR testing

Isotope	Spin	Larmor frequency (MHz)	90° pulse width (μs)	Number of scans	Acquisition time (s)	Relaxation delay (s)
^{7}Li	3/2	155.429	23	200	0.2	1.0
^{23}Na	3/2	105.795	20	500	0.5	0.1
^{133}Cs	7/2	52.462	35	200	0.5	0.2

3.4. Electrical and electromechanical characterizations

The films that were coated with electrodes were characterized for their electromechanical transduction behavior as actuators. For the actuation testing, the films were clamped in a cantilevered configuration and allowed to bend freely. A schematic of the test setup is shown in Fig. 3. The membranes were 0.3 cm wide and 3.5 cm in length, with a free length of 2.5 cm when positioned in the clamp. A step input of 1.5 V was applied across the thickness of the benders and the displacement was measured 1.5 cm from the clamp using a non-contact laser vibrometer. From this measured displacement and the geometry of the benders, the strain generated at the outer surface was computed using

$$\varepsilon = \frac{\delta t}{L_{\mathrm{f}}^{2}} \tag{3}$$

where ε is the strain, δ is the measured displacement, t is the thickness of the bender, and L_{f} is the distance from the clamp to the point at which the displacement was measured (1.5 cm). This equation assumes that the ionomeric polymer actuators bend with a constant curvature. Bar-Cohen and Leary and

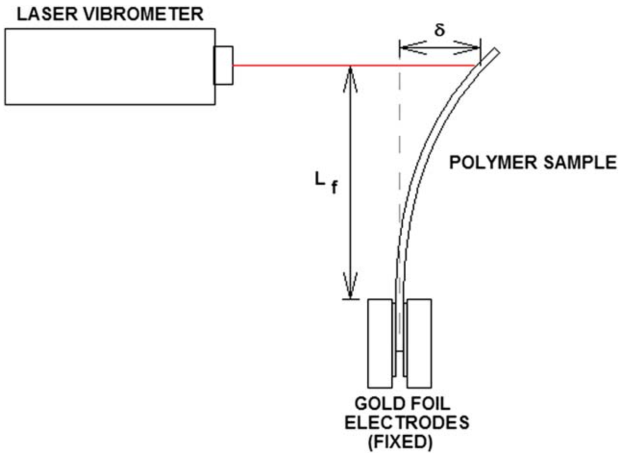

Fig. 3. Experimental setup that was used to characterize the electromechanical transduction behavior of the membranes.

independently Newbury have previously shown this assumption to be reasonable [32,33]. The actuation speed was determined from the step response by measuring the slope of the response with respect to time for the first 20 ms after the step was applied.

The ionic conductivity of the ionic liquid-swollen Nafion films was also measured. For this testing, the same films 0.3 × 3.5 cm were clamped in a cantilevered configuration and excited with a random voltage signal with a frequency bandwidth of 200 Hz and an RMS value of 0.4 V. The current through the actuators was measured by amplifying the voltage drop across a small resistor (0.1 Ω) in series with the membrane. From the measured voltage and current the frequency-dependent impedance of the actuators was determined. Using this impedance and the geometry of the actuators, the ionic conductivity was determined from

$$\sigma = \frac{t}{Rwl} \tag{4}$$

where σ is the ionic conductivity, t is the distance between the electrodes (the thickness of the film), R is a characteristic impedance, w is the width of the film, and l is the length of the film. For this analysis, the average of the electrical impedance over the range 100–200 Hz was used as the characteristic impedance R.

4. Results and discussion

4.1. Small-angle X-ray scattering

Nafion ionomer consists of a Teflon-like backbone with pendant side chains. The sulfonate exchange sites at the ends of these side chains are strongly hydrophilic, whereas the fluorocarbon portion of the polymer is strongly hydrophobic. Therefore, Nafion exhibits a unique morphology, in which these two domains form separated "phases," one that is rich in ionic groups and one that is rich in fluorocarbon polymer. Although the specific morphology of Nafion polymer remains debated, the most generally accepted theory is the cluster-network model first proposed by Gierke et al. [34,35]. In this model, the sulfonate exchange sites and counterions of the polymer reside on the inner surface of ionic clusters that represent inverted micelles. Although this model is likely an oversimplification, it is sufficient for the current discussion. These ionic clusters are thought to be contained within an inert fluorocarbon matrix and interconnected by short, narrow channels – see Fig. 4. It is this conductive cluster network that gives rise to the unique transport properties of Nafion.

Other researchers have proposed alternative theories of the morphology of Nafion. Hashimoto et al. have suggested that the morphology of Nafion may also be described by a core–shell model, in which ion-rich clusters are surrounded by a fluorocarbon phase and embedded in an intermediate ionic phase that contains both fluorocarbon polymer and non-clustered ionic sites [36]. Yeager and Steck have proposed a model that in spirit is similar to Gierke's cluster-network model [37]. However, they remove the constraint that the clusters be spherical and introduce a third intermediate phase between the ion-rich clusters and the inert fluorocarbon matrix. This is likely the most realistic interpretation of the microstructure of Nafion.

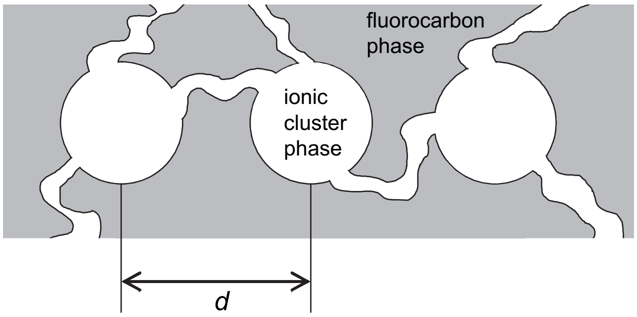

Fig. 4. The cluster-network model first proposed by Gierke et al. [34,35].

Small-angle X-ray scattering (SAXS) has been the most commonly used technique to investigate the clustered morphology in water-swollen Nafion [35,38]. Three prominent features are observed in the SAXS data for Nafion: the so-called ionomer peak, an upturn at small angles, and a broad shoulder associated with crystallites in the Teflon-like fluorocarbon phase. Based on the cluster-network model proposed by Gierke and to a lesser extent the three-phase model proposed by Yeager and Steck, the angular position of the ionomer peak is thought to correspond to the mean center-to-center spacing between the ionic clusters (d). The small-angle upturn is believed to be associated with long-range inhomogeneity in the spatial distribution of the clusters [39–41]. Gierke et al. observed that the mean intercluster spacing increases with increasing water content [35]. Because water is excluded from the highly hydrophobic fluorocarbon phase, it can only swell the hydrophilic ionic clusters. Therefore, the increase in the mean intercluster spacing corresponds to an increase in the mean size of the clusters. Gierke et al. also argued that swelling of the clusters may be associated with coalescence of adjacent clusters. By this argument, absorption of water into a Nafion membrane would also result in a decrease in the number density of the clusters.

In the present work, SAXS has been performed on Nafion membranes swollen with EMI-Tf and EMI-Im ionic liquids. The results of this testing are presented in detail by Bennett [42] and Bennett and Leo [43]. Similar to the results of Gierke et al., the mean intercluster spacing was found to increase with increasing content of ionic liquid. The mean intercluster spacing was also observed to be larger for the membranes swollen with the EMI-Tf ionic liquid than for those swollen with the EMI-Im ionic liquid. This increase is though to arise from an increase in the size of the clusters, both by swelling and by aggregation of adjacent clusters. More importantly, the SAXS result was found to depend strongly on the structure and properties of the ionic liquid. This is evident in Fig. 5. As can be seen, the two features associated with the presence of the ionic clusters (the ionomer peak and the small-angle upturn) are notably absent for the membrane swollen with the

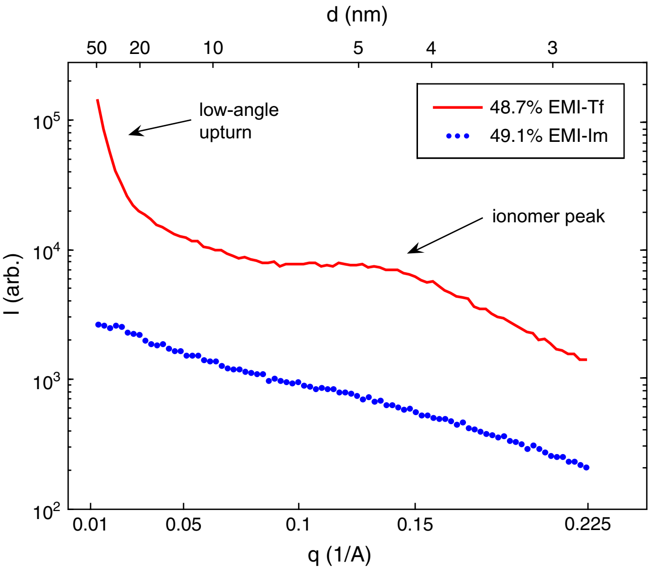

Fig. 5. Comparative SAXS result for Nafion membranes swollen with both ionic liquids. The uptake of ionic liquid is reported as a percentage of the dry volume.

EMI-Im ionic liquid. This suggests that the clustered morphology of the membrane is disrupted by the presence of the EMI-Im ionic liquid. This can be explained by considering that the EMI-Tf ionic liquid is water miscible, whereas the EMI-Im ionic liquid is hydrophobic (see Table 1). Therefore, the EMI-Tf ionic liquid is most likely absorbed into the clusters and excluded from the fluorocarbon phase, much like water. However, the EMI-Im ionic liquid is likely incorporated at least partially into the fluorocarbon matrix of the Nafion polymer. This is reasonable considering that the EMI-Im ionic liquid is highly fluorinated (see Fig. 2) and hydrophobic and should be compatible with the fluorocarbon phase. This incorporation would result in partial homogenization of the membrane, which is consistent with the SAXS results. This would also lead to the interruption of the connectivity of the ionic cluster network, thus diminishing the ionic conductivity of the membrane.

4.2. Fourier transform infrared spectroscopy

Of critical importance in this research is the identification of the prevalent ion associations within ionic liquid-swollen Nafion membranes. One of the most useful tools available to probe these associations is infrared spectroscopy. For this work, attenuated total reflectance (ATR) spectroscopy was used. Several researchers have performed FTIR studies of Nafion membranes and have concluded that the peak that is observed near 1060 cm^{-1} in the spectrum corresponds to the symmetric stretching vibration of the sulfonate exchange sites [44–46]. In 1980, Lowry and Mauritz performed a detailed analysis of this peak as the water content and counterion of the polymer were varied [46]. They observed that the symmetric sulfonate stretching peak shifted to lower wavenumbers (lower vibrational frequency) as the size of the counterion was increased and as the content of water within the membrane was increased. This shift corresponds to a decrease in the polarization of the S–O dipole resulting from increased separation between the counterion and the exchange site. This increased separation can be caused by increased size of the counterion or by hydration of the ions with water.

At low water contents, Lowry and Mauritz found the symmetric sulfonate stretching peak to exhibit a linear dependence on the water content. However, at high water content, the symmetric sulfonate stretching peak was observed to be constant and was to occur very near 1058 cm^{-1} for all counterion forms of the membrane [46]. This finding has been confirmed by a number of other researchers [44,45]. This indicates that for the highly swollen membranes, the proximity of the counterions to the exchange sites is independent of water content. It is also interesting that the water content at which this transition occurred was lower for the membranes exchanged with larger counterions. This indicates that the larger counterions are more easily displaced from the exchange sites and is reasonable considering that the electrostatic energy binding the counterions to the exchange sites is related to the interionic distance by an inverse square law. That is, the larger counterions are less tightly bound to the sulfonate exchange sites.

In the current study, attenuated total reflectance (ATR) spectroscopy experiments were performed on ionic liquid-swollen Nafion films that were prepared as described in Section 2. Portions of the IR spectra for six Nafion membranes in the sodium cation form and swollen with varying amounts of EMI-Tf ionic liquid are shown in Fig. 6. As can be seen, the symmetric sulfonate stretching frequency of the Nafion membrane, near 1060 cm^{-1}, shifts to lower wavenumbers as the content of ionic liquid is increased. Also evident in this figure is a peak associated with the symmetric sulfonate stretching frequency of the trifluoromethanesulfonate anion of the EMI-Tf ionic liquid, which also shifts to lower wavenumbers with increased swelling. From the ATR results, the shift in these peaks was monitored over a range of experimental

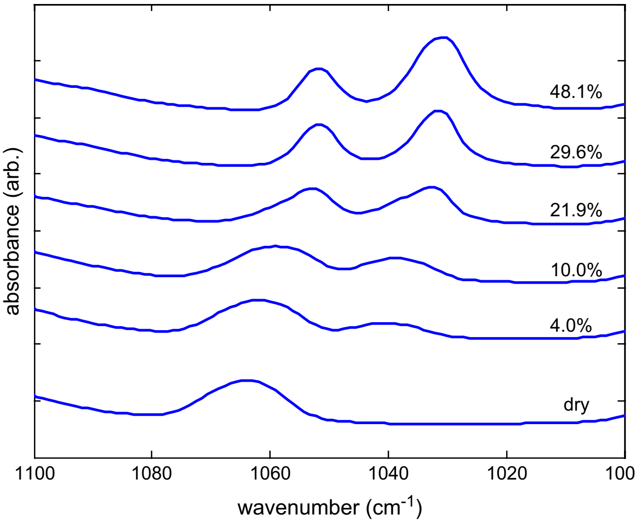

Fig. 6. IR spectra for Nafion membranes exchanged into the sodium cation form and swollen with EMI-Tf ionic liquid. All loadings are reported as a percentage of the dry membrane volume.

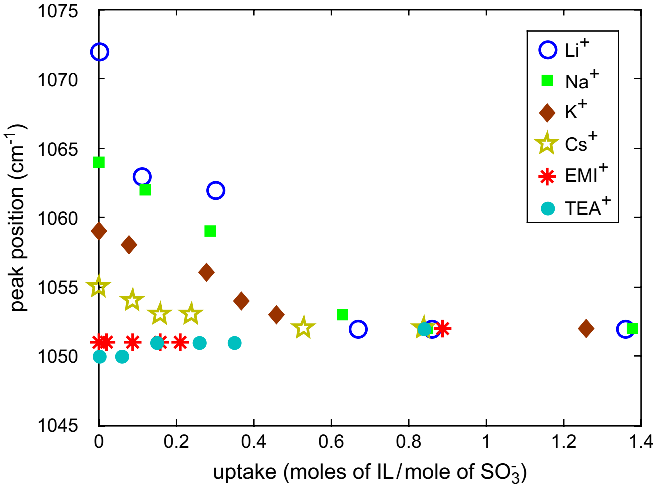

Fig. 7. Symmetric sulfonate stretching vibration of the Nafion membrane versus the loading of EMI-Tf ionic liquid.

parameters. Plotted in Fig. 7 is the position of the symmetric sulfonate stretching peak associated with the Nafion polymer versus the uptake of EMI-Tf ionic liquid for six cation forms of the membrane. The counterion sizes are listed in Table 3. As can be seen, the peak position shifts to higher wavenumbers (higher frequency) with decreasing size of the counterion, for the dry membranes. Also, for most of the cations, the frequency decreases with increasing content of ionic liquid until a critical loading of ionic liquid. Above this critical loading the frequency remains constant. The shape of the curves is very similar to those observed by Lowry and Mauritz. Above the transition, the sulfonate symmetric stretching peak is located at 1052 cm^{-1} for all cation forms of the membrane. This is lower than the frequency of 1058 cm^{-1} that has been observed in water-swollen Nafion membranes. Also, for the EMI$^+$ and TEA$^+$ ions, the frequency actually increases with increased loading of ionic liquid, more so for the TEA$^+$ ion. The smallest shift in frequency is observed for the membranes in the EMI$^+$ ion form.

As with the hydrated membranes, the decrease in the symmetric sulfonate stretching frequency corresponds to a decrease in the polarization of the S—O dipole. This is caused by an increase in the distance between the counterion and the exchange site. For the EMI-Tf-swollen membranes, the decreased polarization is believed to be caused by the displacement of the counterion of the membrane away from the sulfonate site by the EMI$^+$ cation of the ionic liquid. For the smaller lithium, sodium, and potassium ions, this exchange results in an increase in the size of the ion associated with the exchange site. Because the TEA$^+$ ion is larger than the EMI$^+$ ion, this exchange has the opposite effect. The decrease in the size of the ion associated with the exchange site results in an increase in the polarization of the S—O dipole. This is why the frequency of the SO_3^- group was observed to increase when the TEA-exchanged membranes were swollen with the EMI-Tf ionic liquid. This argument is supported by the fact that the shift in the symmetric sulfonate stretching frequency was observed to be the smallest for the EMI-exchanged membranes.

Table 3
Critical uptake of EMI-Tf ionic liquid for Nafion membranes in six different counterion forms as determined by FTIR

Cation	Radius (nm)	Critical uptake (mol IL/mol SO_3^-)
Li$^+$	0.59[a]	0.66
Na$^+$	0.99[a]	0.69
K$^+$	1.37[a]	0.56
Cs$^+$	1.67[a]	0.48
EMI$^+$	3.04[b]	0.45
TEA$^+$	3.20[c]	0.44

[a] From Ref. [47].
[b] Calculated from the volume cited in Ref. [48].
[c] Calculated from the volume cited in Ref. [49].

It is interesting to note that the curves in Fig. 7 exhibit an inflection point, just as in the results of Lowry and Mauritz. In this work, the loading of ionic liquid at which this inflection point occurs is defined as the "critical uptake" and is believed to correspond to the minimum amount of ionic liquid required to displace essentially all of the counterions away from the sulfonate exchange sites. As can be seen in Fig. 7, the critical uptake decreases with increasing size of the counterion. In order to estimate the critical uptake from the FTIR data, the symmetric sulfonate stretching frequency was assumed to exhibit a linear dependence on the loading of ionic liquid below the critical uptake. Based on this assumption, straight lines were fit to the data below the critical uptake. The slope (m) and y-intercept (b) obtained from these linear fits were then used to determine the critical uptake of ionic liquid from

$$f_c = \frac{(1052 - b)}{m} \qquad (5)$$

where f_c is the critical uptake of EMI-Tf ionic liquid determined from the FTIR results and 1052 cm^{-1} is the saturation value of the symmetric sulfonate stretching peak above the critical uptake. Using this method, the critical uptake for the alkali metal ions was determined and is presented in Table 3. This method was also used to determine the critical uptake for the TEA form membranes. For the EMI form membranes, the shift in the symmetric sulfonate stretching frequency was only 1 cm^{-1} over the entire swelling range. Also, for those membrane, no data points were obtained in the swelling range 0.3—0.8 mol/mol. For these reasons, the line-fitting method described could not be used to determine the critical uptake for the EMI form membranes. However, from Fig. 7 and the trend exhibited by the data in Table 3, it was estimated to be 0.45 mol/mol. The observed trend of decreasing critical uptake with increasing size of the counterions is due to a decrease in the electrostatic binding energy between the counterions and the exchange sites as the size of the counterions is increased. Therefore, less ionic liquid is required to displace the larger counterions from the sulfonate sites. This trend is in agreement with the findings of Lowry and Mauritz.

Because the EMI-Tf ionic liquid contains a sulfonate site, the IR spectra also contained a peak associated with the symmetric sulfonate stretching vibration of the ionic liquid within the membranes; this can be seen in Fig. 6. The position of this peak was monitored as the counterion and content of ionic liquid were varied – see Fig. 8. At low loadings of ionic liquid, the symmetric sulfonate stretching vibration of the ionic liquid was observed to be higher for the membranes exchanged with smaller counterions. This can be explained by considering that the counterions displaced by the EMI^+ cations become associated with the trifluoromethanesulfonate (Tf^-) anions of the ionic liquid. Because these smaller counterions have a higher polarizing effect on the Tf^- anion than the EMI^+ cation does, the symmetric sulfonate stretching frequency increases. Above the critical uptake of ionic liquid, the symmetric sulfonate stretching frequency of the ionic liquid was observed to be 1031 cm^{-1}. This corresponds to the peak position that was measured for the neat ionic liquid, by spreading a small drop of EMI-Tf over the ATR crystal. This indicates that above the critical uptake, all of the counterions have been displaced from the sulfonate exchange sites and a large amount of "free" ionic liquid exists within the membrane. The critical uptake of EMI-Tf ionic liquid determined from observations of the symmetric sulfonate stretching frequency of the ionic liquid was found to be in good agreement with the results presented in Table 3. FTIR studies were also performed on membranes swollen with the EMI-Im ionic liquid. However, the EMI-Im ionic liquid was found to contain a peak in the infrared spectrum that obscured the peak of interest at 1060 cm^{-1}. No reliable conclusions could be drawn from the data as the two peaks could not be distinguished.

4.3. Nuclear magnetic resonance spectroscopy

Nuclear magnetic resonance (NMR) spectroscopy is a useful tool for probing the local electronic environment of individual nuclei. Komoroski and Mauritz have previously shown that alkali metal NMR can be used to make determinations of the mobility of alkali metal counterions within Nafion [50,51]. They observed a decrease in the NMR peak width as the content of water within the polymer was increased, for Nafion in the lithium, sodium, and cesium counterion forms. The peak width is related to the speed at which the transverse magnetization of the sample relaxes. There are numerous mechanisms by which magnetization in a sample can relax, including spin–rotation coupling, dipole–dipole coupling, shielding anisotropy, and scalar coupling [52]. However, for nuclei that possess spins greater than 1/2, relaxation by nuclear quadrupolar coupling is often several orders of magnitude faster than any other mechanism [52]. The strength of this relaxation mechanism is related to the electric quadrupole moment of the nucleus, the electric field gradient in the vicinity of the nucleus, and the mobility of the molecule. Common factors affecting the mobility of molecules within a material are temperature, viscosity, and molecular size. Komoroski and Mauritz have observed the ^{23}Na peak width to decrease from about 4000 Hz in a dry polymer to less than 500 Hz when the polymer was highly swollen with water [51]. This is related to an increase in the mobility of the sodium ions. They have also observed that the ^{23}Na peak width of Nafion swollen with 5% water (by weight) decreased by almost half (from 1100 Hz to 600 Hz) when the temperature was increased from 30 °C to 90 °C. This is due to an increase in the mobility of the sodium ions with increasing temperature. As with the FTIR results of Lowry and Mauritz, the NMR peak width observed by Komoroski and Mauritz was found to be strongly dependent on hydration at low water contents. However, for high water contents, the peak width was found to be relatively constant. The water content at which this transition occurred was observed to decrease with increasing size of the counterions. Again, this indicates that larger counterions are more easily displaced from the sulfonate exchange sites.

For the current study, alkali metal NMR was performed on samples of Nafion-117 membranes that were exchanged into the lithium, sodium or cesium counterion form and swollen to various levels with EMI-Tf and EMI-Im ionic liquids. The purpose of these experiments was to evaluate the mobility of the Li^+, Na^+, and Cs^+ ions within the membranes as a function of the uptake of ionic liquid and relate this mobility to the properties of the ionic liquid. The ^{23}Na NMR peak width for ionic liquid-swollen Nafion films is plotted versus the uptake of ionic liquid in Fig. 9. The shape of these curves is in agreement with the results of Komoroski and Mauritz. The decrease in the peak width at low swelling levels is related to an increase in the mobility of the sodium counterions. As the content of ionic liquid is increased, more and more of the counterions are displaced from the exchange sites and associated with the trifluoromethanesulfonate anions of the EMI-Tf ionic liquid. The mobility of the counterions is increased by this exchange because the Tf^- anions are more mobile than the fixed sulfonate exchange sites, which are covalently bound to the polymer backbone. As with the FTIR results, the NMR data for the EMI-Tf-swollen membranes exhibit an inflection point above which the peak width is relatively constant. Using the same technique that was used for the FTIR results, the critical uptake of EMI-Tf ionic liquid was determined from the NMR data shown in Fig. 9 to be 0.65 mol of ionic liquid per

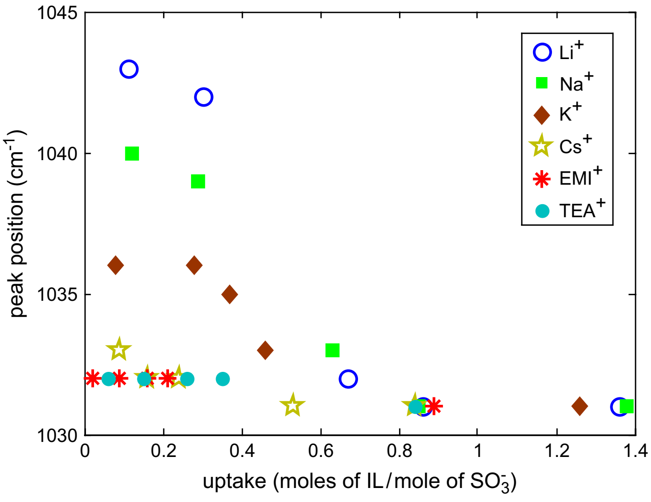

Fig. 8. Symmetric sulfonate stretching vibration of the trifluoromethanesulfonate anion versus the loading of EMI-Tf ionic liquid.

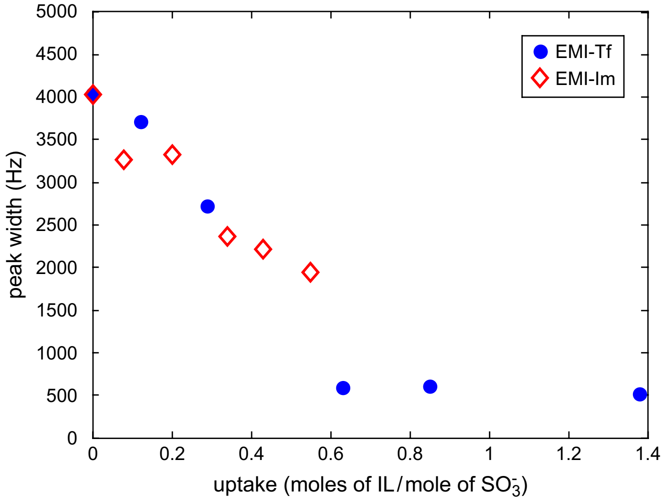

Fig. 9. ^{23}Na NMR peak width at half height for sodium-exchanged Nafion membranes swollen with both ionic liquids.

mole of exchange sites. This is in good agreement with the value of 0.69 mol/mol that was determined from the FTIR analysis for the sodium-form membranes.

It is interesting to note that the ^{23}Na peak width is larger for the membranes swollen with the EMI-Im ionic liquid than for those swollen with the EMI-Tf ionic liquid. This indicates that the sodium ions are more mobile within the EMI-Tf-swollen membranes. This is perhaps surprising considering that the EMI-Im ionic liquid is actually *less* viscous than the EMI-Tf ionic liquid (see Table 1). This finding can be most reasonably explained by considering the SAXS results. From these findings it was proposed that the EMI-Im ionic liquid resulted in disruption of the clustered morphology of the Nafion polymer. This disruption interrupts the connectivity of the conductive cluster network and inhibits the mobility of the counterions within the membrane, which is consistent with the NMR results.

In addition to sodium, NMR investigations were also performed on lithium- and cesium-exchanged membranes. The results of these investigations will be summarized; details may be found elsewhere [42]. The ^{7}Li NMR peak width was measured for lithium-form membranes swollen with the EMI-Tf and EMI-Im ionic liquids. As with the ^{23}Na results, the ^{7}Li NMR peak width was observed to decrease with increasing content of ionic liquid, at low swelling levels. Above the critical uptake, the peak width was found to be relatively constant. The peak width was larger for the membranes swollen with the EMI-Im ionic liquid (1900 Hz at 0.90 mol/mol uptake) than for those swollen with the EMI-Tf ionic liquid (126 Hz at 0.86 mol/mol uptake). Although there were insufficient data to perform the line-fitting procedure described previously, the critical uptake of EMI-Tf ionic liquid was qualitatively in agreement with the FTIR results, as an inflection point was observed at approximately 0.7 mol/mol. The ^{133}Cs results were similar. Again, the peak width was larger for the EMI-Im-swollen membranes (3100 Hz at 0.33 mol/mol uptake) than for the EMI-Tf-swollen membranes (1800 Hz at 0.24 mol/mol uptake). This indicates that the cesium ions are more mobile in the membranes swollen with the EMI-Tf ionic liquid and is likely related to the disrupting effect that the EMI-Im ionic liquid has on the clustered morphology of the Nafion polymer. Using the line-fitting technique, the critical uptake of EMI-Tf ionic liquid for the cesium-form membranes was determined to be 0.46 mol/mol. This is in good agreement with the value of 0.48 mol/mol that was determined from the FTIR analysis.

4.4. Characterization of electromechanical transduction

In addition to the SAXS, FTIR, and NMR testing, the ionic liquid-swollen Nafion membranes were also characterized for their transduction behavior. This testing involved the measurement of the ionic conductivity and actuation speed of the transducers. The ionic conductivity was determined from the measured electrical impedance through the thickness of the films using the method described in Section 3. In order to validate the use of this method for making determinations of ionic conductivity, the results were compared to measurements made using the more common method described by Zawodzinski et al. [53]. In this case, unplated Nafion membranes were positioned in a fixture in contact with two brass electrodes such that the current flow was in the planar direction of the films. An HP impedance analyzer was used to measure the complex impedance of the films, which was displayed on a Nyquist plot (real component on the *x*-axis, imaginary component on the *y*-axis). According to the method of Zawodzinski et al., the characteristic impedance used to compute the ionic conductivity was taken to be the magnitude of the real part of the impedance when the imaginary part was at a minimum. The ionic conductivity was then calculated using Eq. (4), where t is 3.25 mm, w is 32 mm, and l is the measured thickness of the film. The ionic conductivity for Nafion membranes in the lithium ion form and swollen with EMI-Tf ionic liquid determined using both techniques is shown in Fig. 10. As can be seen, good agreement is exhibited between the two methods.

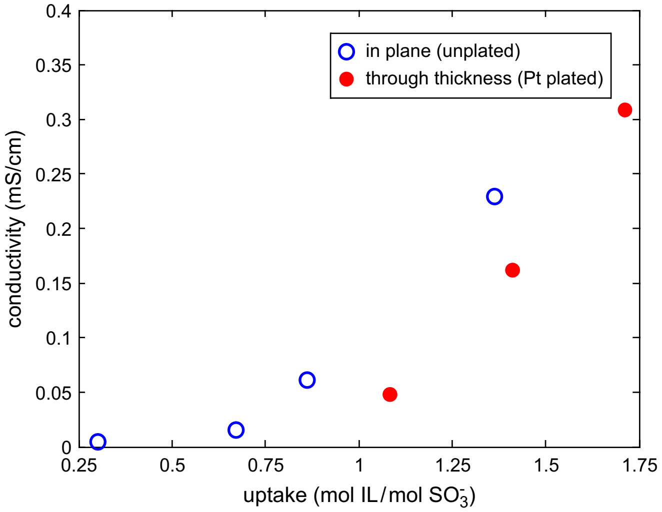

Fig. 10. Ionic conductivity determined by through-thickness measurements on platinum-plated membranes and by measurements in the plane of unplated membranes. The counterion is lithium and the ionic liquid is EMI-Tf.

It is evident from Fig. 10 that the ionic conductivity measured for the platinum-plated samples is lower than that measured for the unplated samples. This can be explained by considering that the ionic conductivity exhibited by Nafion membranes is anisotropic. This anisotropy is likely introduced as a result of processing of the films during manufacture. Evidence for this is provided by the findings of Gebel et al., which revealed the swelling process of Nafion membranes with a diluent to be anisotropic [54]. Also, Mueller has found the proton conductivity and diffusion coefficient of Nafion-117 membranes to be higher in the planar direction than in the thickness direction [55]. These findings are consistent with the results of the current study. Additional evidence is provided by Rollet et al. [56]. They determined that the diffusion coefficient for sodium ions within a sulfonated polyimide membrane was higher in the planar direction than in the thickness direction. Both Mueller and Rollet et al. supported their conclusions with NMR and conductivity measurements and both attributed the difference in the observed conductivities to anisotropy of the films.

It is also interesting to note that the ionic conductivity measured for the unplated films exhibits an inflection point at an uptake of 0.67 mol/mol. This is consistent with the FTIR results, in which the critical uptake for lithium-form membranes swollen with EMI-Tf ionic liquid was found to be 0.66 mol/mol. This result is a further evidence that the properties and behavior of the membranes undergo a change at the critical uptake of ionic liquid.

The response speed versus the uptake of ionic liquid for the platinum-plated actuators was also measured and is shown in Fig. 11. As can be seen, the actuation speed increases with increasing uptake of ionic liquid. Furthermore, the EMI-Tf-swollen actuators exhibit a much faster response than the EMI-Im-swollen actuators. The actuation speed also increases with increasing size of the counterions, for both ionic liquids. A similar trend is observed for the ionic conductivity – see Fig. 12. As can be seen, the ionic conductivity of the EMI-Tf-swollen membranes is higher than the EMI-Im-swollen membranes. Also, the ionic conductivity increases with increasing size of the counterions. If the actuation speed is plotted versus the ionic conductivity, a clear trend is observed – see Fig. 13. As can be seen, the actuation speed is linearly related to the ionic conductivity. This result supports the notion that actuation of the polymer is caused by charge motion and indicates that both of these metrics are related to the mobility of the ions.

It is interesting to note that the charge mobility is higher for the membranes swollen with the EMI-Tf ionic liquid than for those swollen with the EMI-Im ionic liquid, considering that the EMI-Im ionic liquid actually has a lower viscosity. This is consistent with the alkali metal NMR results in which the peak width was observed to be larger for those membranes swollen with the EMI-Im ionic liquid than those swollen with the EMI-Tf ionic liquid, even at equivalent swelling levels. These differences can be explained by considering the effect that the EMI-Im ionic liquid has on the morphology of the Nafion membranes. The SAXS results indicated that the EMI-Im ionic liquid led to partial homogenization of the membrane and decreased the contrast between the fluorocarbon and ionic cluster phases. This mixing of the phases interrupts the connectivity of the ionic cluster network and inhibits ion mobility within the membrane. Also, from the ionic conductivity and actuation speed results, the ion mobility increases with increasing size of the counterions, which corresponds to decreasing critical uptake. This relationship will form the basis of a model of charge transport in the ionic liquid-swollen membranes.

5. Development of the charge transport model

In order to understand why the charge mobility increases with increasing size of the counterions and increasing content of ionic liquid, a model of charge transport within the ionic liquid-swollen membranes is developed. As observed by the

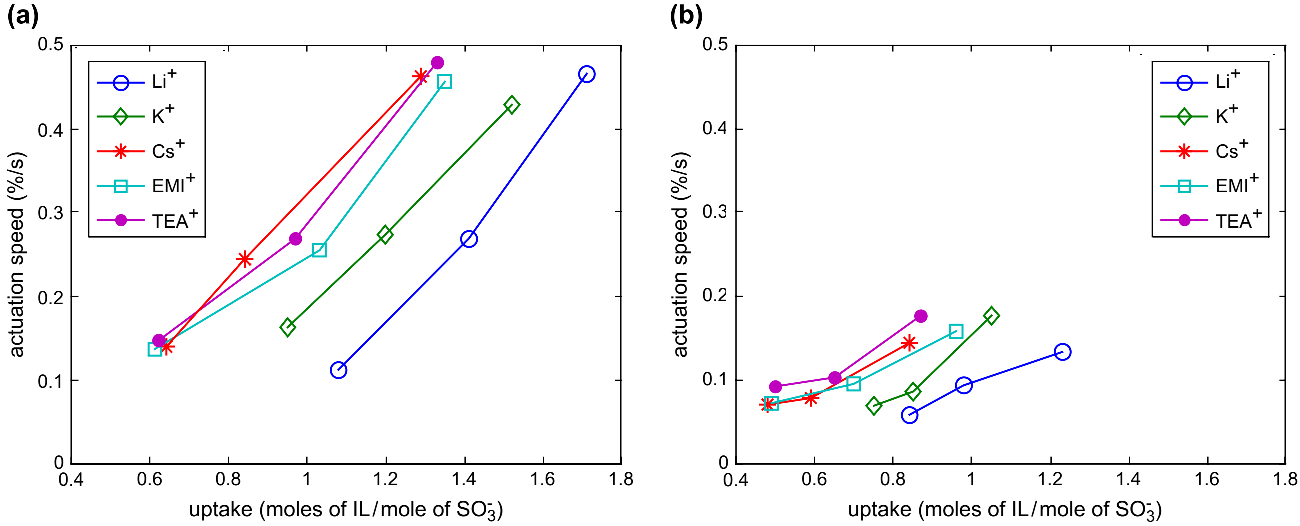

Fig. 11. Actuation speed for the platinum-plated membranes versus uptake of ionic liquid for (a) EMI-Tf and (b) EMI-Im.

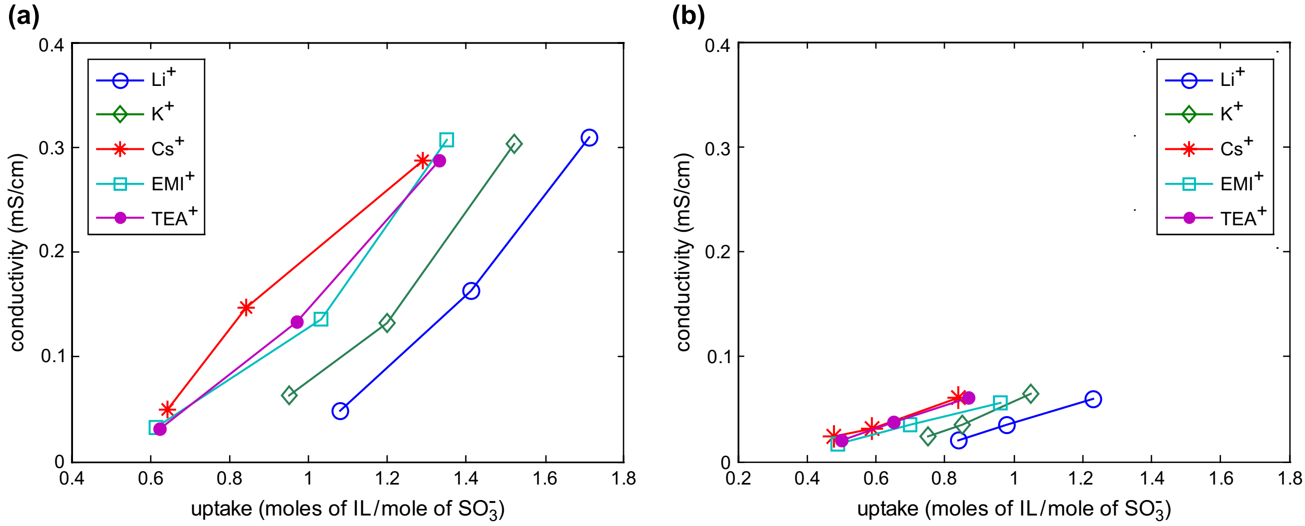

Fig. 12. Ionic conductivity for the platinum-plated membranes versus uptake for (a) EMI-Tf and (b) EMI-Im.

FTIR and NMR results, a critical uptake of ionic liquid exists above which the properties of the membrane undergo a transition. For the EMI-Tf ionic liquid, it is argued that the EMI^+ cation interacts with the polymer by displacing the counterions away from the exchange sites. As the counterions are displaced, they associate with the Tf^- anions of the ionic liquid. The critical uptake is believed to correspond to the minimum amount of ionic liquid required to displace essentially all of the counterions. Above the critical uptake, additional ionic liquid is present within the membrane that does not interact with the counterions or exchange sites. Because this "free" ionic liquid contains Tf^- anions that are only loosely associated with EMI^+ cations, these anions represent sites that can be occupied by a counterion of the polymer. It is by hopping among these Tf^- sites that the counterions are believed to transport within the ionic liquid-swollen Nafion membranes. Therefore, the model predicts that the counterions of the Nafion polymer are the primary charge carriers in the ionic liquid-swollen membranes. As the amount of free ionic liquid within the membrane is increased, the number of available sites is increased and the mobility of the counterions is enhanced. Therefore, the key parameter of this model is the *content of ionic liquid above the critical uptake*. The FTIR and NMR results revealed that the critical uptake decreases with increasing size of the counterions. Thus, for the membranes exchanged with larger counterions, the transition from insulator to conductor occurs at a lower loading of ionic liquid. This is why the charge mobility is observed to increase with increasing counterion size, for a given swelling level.

In order to test this model, the actuation speed is plotted versus the uptake of ionic liquid normalized by the critical uptake – see Fig. 14. It should be noted that the critical uptake was determined *from the spectroscopy experiments*. As can be seen, the data exhibit a single universal trend. This supports the argument that the key model parameter is the loading of ionic liquid above the critical uptake. However, based on the

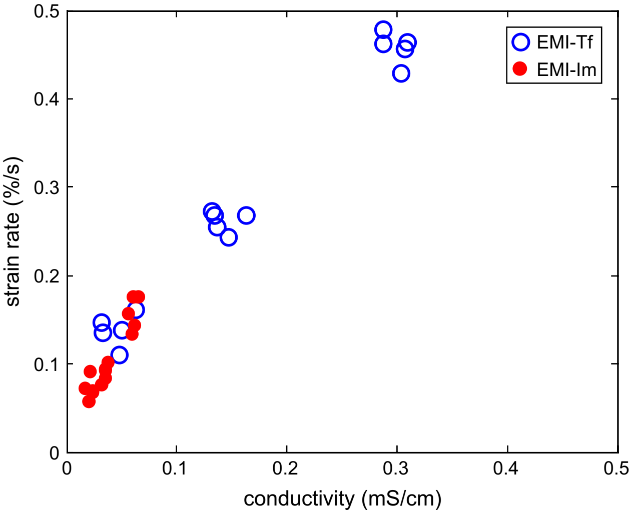

Fig. 13. Actuation speed versus ionic conductivity for the platinum-plated membranes swollen with both ionic liquids.

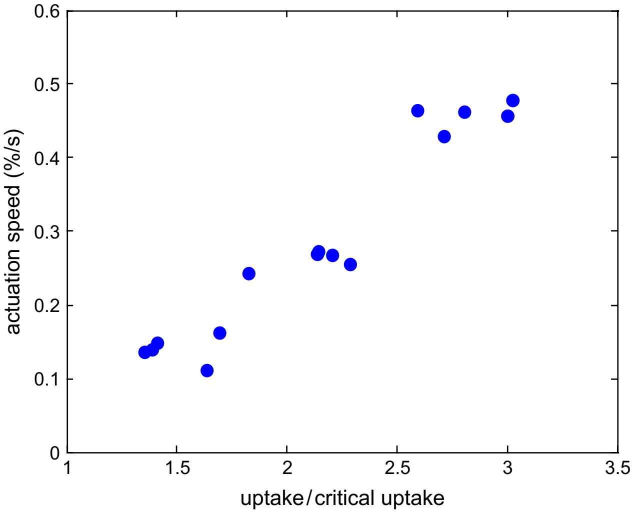

Fig. 14. Actuation speed versus uptake of EMI-Tf ionic liquid normalized by the critical uptake for the platinum-plated samples in five counterion forms.

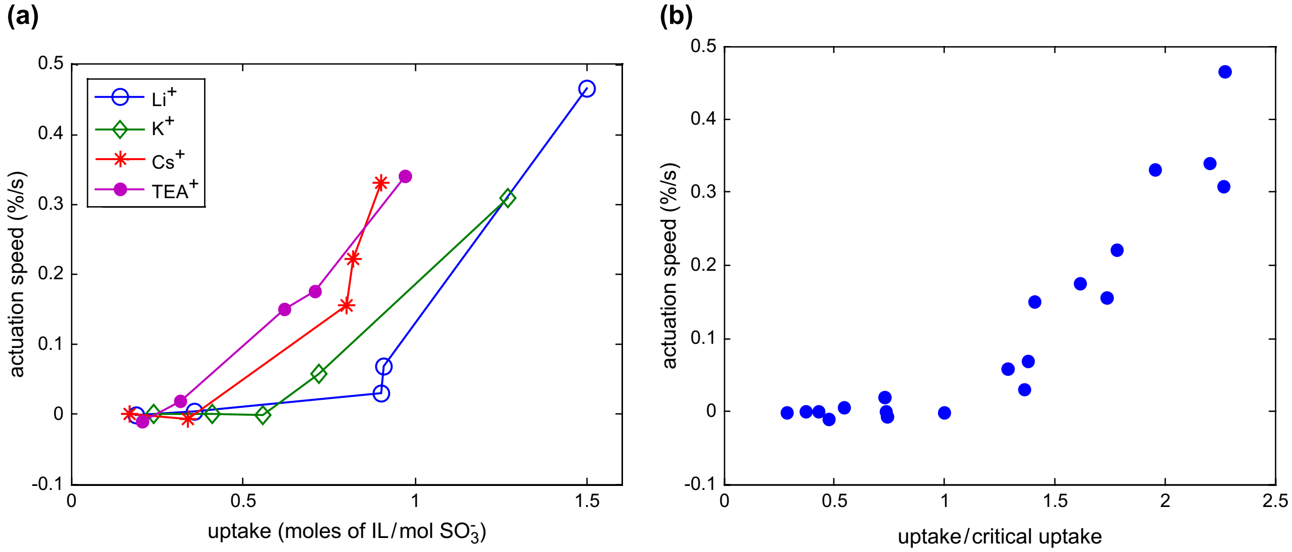

Fig. 15. (a) Actuation speed versus uptake of EMI-Tf ionic liquid for the RuO_2-plated actuators and (b) actuation speed versus uptake normalized by the critical uptake.

proposed model, this curve should exhibit an inflection point at a loading of 1.0. For the platinum-plated samples, this inflection point is not observed because no data points were taken below the critical uptake. As further support of the model, additional testing was performed using samples that were plated with RuO_2 by the direct assembly method, as described in Section 2. These samples were tested in exactly the same manner as the platinum-plated transducers. The actuation speed versus the uptake of EMI-Tf ionic liquid for the RuO_2-plated samples is shown in Fig. 15a. As can be seen, the actuation speed increases with increasing size of the counterions, for a given loading of ionic liquid. The curves are also observed to exhibit an inflection point at the critical uptake of ionic liquid. These data were plotted versus the uptake normalized by the critical uptake in order to test the validity of the model. Again, the critical uptake was determined from the FTIR and NMR results using a different set of membranes. As can be seen in Fig. 15b, a single relationship is observed that exhibits an inflection point at a loading of 1.0. This additional evidence is a further support of the proposed model of charge transport.

Although the charge transport model was developed using the results for the EMI-Tf-swollen membranes, one would expect the same mechanism to be present in the EMI-Im-swollen membranes. Unfortunately, insufficient data exist to test this theory. It is clear that the charge mobility is higher for the membranes swollen with the EMI-Tf ionic liquid, however. As previously stated, this is believed to be related to the disruption of the ionic cluster network within the Nafion polymer by the EMI-Im ionic liquid.

6. Conclusions

Ionic liquids may be used effectively to replace water in Nafion membrane transducers. Small-angle X-ray characterization of ionic liquid-swollen Nafion membranes revealed that the structure of the ionic liquid has a profound effect on morphology of the films. Membranes swollen with the hydrophobic EMI-Im ionic liquid exhibited more homogeneous morphology, with less distinct ionic cluster regions. The belief that this effect inhibits charge transport was supported by the results of NMR, actuation, and conductivity testing. Infrared spectroscopy revealed that the ionic liquid interacts with the Nafion polymer by displacing the counterions away from the sulfonate exchange sites. From NMR testing, it is clear that this displacement leads to an increase in the mobility of the counterions. The FTIR and NMR results exhibit an inflection point at the critical uptake of ionic liquid. This is thought to be the minimum content of ionic liquid required to displace all of the counterions. The critical uptake decreases as the size of the counterions increases, because the larger counterions are more easily displaced. Electromechanical characterization of these membranes reveals that the actuation speed and ionic conductivity increase with increasing counterion size and increasing content of ionic liquid. Based on the observed trends, a model is formulated to explain the charge transport mechanisms within the ionic liquid-swollen films. In this model, the counterions of the polymer are thought to be the primary charge carriers. The critical parameter of this model is the content of ionic liquid above the critical uptake. In order to test this model, the actuation speed was plotted versus the uptake of ionic liquid normalized by the critical uptake — a single relationship was observed. The elegance of this model is that it combines the results of morphological, spectroscopic, and macroscopic transduction characterizations in a single unified theory of charge transport in ionic liquid-swollen Nafion membranes.

Acknowledgements

This work was supported by the U.S. Army Research Laboratory and U.S. Army Research Office under contract/grant number DAAD19-02-1-0275 Macromolecular Architecture for Performance (MAP) MURI. Supplementary funding was provided by the Virginia Space Grant Consortium. The authors would like to thank Tom Glass of the Virginia Tech Chemistry Department for valuable assistance with the NMR testing.

References

[1] Kuhn W. Reversible dehung und kontraktion bei anderung der ionisation eines netzwerks polyvalenter fadenmolekulionen. Experientia 1948;5: 318–9.

[2] Kuhn W, Hargitay B, Katchalsky A, Eisenberg H. Reversible dilation and contraction by changing the state of high-polymer acid networks. Nature 1950;165:514–6.

[3] Katchalsky A. Rapid swelling and deswelling of reversible gels of polymeric acids by ionization. Experientia 1948;5:318–9.

[4] Sadeghipour K, Salomon R, Neogi S. Development of a novel electrochemically active membrane and 'smart' material based vibration sensor/damper. Smart Materials and Structures 1992;1:172–9.

[5] Oguro K. Actuator element. U.S. Patent 5,268,082; 1993.

[6] Shahinpoor M, Bar-Cohen Y, Simpson J, Smith J. Ionic polymer–metal composites (IPMCs) as biomimetic sensors, actuators and artificial muscles – a review. Smart Materials and Structures 1998;7(6):R15–30.

[7] Mallavarapu K, Leo DJ. Feedback control of the bending response of ionic polymer actuators. Journal of Intelligent Material Systems and Structures 2001;12:143–55.

[8] Kothera CS, Leo DJ. Bandwidth characterization in the micropositioning of ionic polymer actuators. Journal of Intelligent Material Systems and Structures 2005;16:3–13.

[9] Mojarrad M, Shahinpoor M. Ion-exchange–metal composite sensor films. In: Smart Materials and Structures, vol. 3042. SPIE; 1997. p. 52–60.

[10] Keshavarzi A, Shahinpoor M, Kim KJ, Lantz J. Blood pressure, pulse rate, and rhythm measurement using ionic polymer–metal composites sensors. In: EAP actuators and devices, vol. 3669. SPIE; 1999. p. 369–76.

[11] Newbury K, Leo DJ. Mechanical work and electromechanical coupling in ionic polymer bender actuators. In: Proceedings of the ASME international mechanical engineering conference and exposition. ASME; 2001. paper AD-23705.

[12] Newbury K, Leo DJ. Chemoelectric and electromechanical modeling of ionic polymer materials. In: 12th International conference on adaptive structures and technologies; 2001. p. 220–31.

[13] Bar-Cohen Y, Leary S, Shahinpoor M, Harrison J, Smith J. Flexible low-mass devices and mechanisms actuated by electroactive polymers. In: EAP actuators and devices, vol. 3669. SPIE; 1999. p. 51–6.

[14] Bar-Cohen Y, Leary S, Shahinpoor M, Harrison JO, Smith J. Electroactive polymer (EAP) actuators for planetary applications. In: EAP actuators and devices, vol. 3669. SPIE; 1999. p. 57–63.

[15] Franklin JW. Electromechanical modeling of encapsulated ionic polymer transducers. Master's thesis, Virginia Tech; 2003.

[16] Bennett M, Leo D. Ionic liquids as stable solvents for ionic polymer transducers. Sensors and Actuators A: Physical 2004;115:79–90.

[17] Lu W, Fadeev AG, Qi B, Smela E, Mattes BR, Ding J, et al. Use of ionic liquids for π-conjugated polymer electrochemical devices. Science 2002;297:983–7.

[18] Ding J, Zhou D, Spinks G, Wallace G, Forsyth S, Forsyth M, et al. Use of ionic liquids as electrolytes in electromechanical actuator systems based on inherently conducting polymers. Chemistry of Materials 2003;15: 2392–8.

[19] Vidal F, Plesse C, Teyssié D, Chevrot C. Long-life air working conducting semi-ipn/ionic liquid based actuator. Synthetic Metals 2004;142: 287–91.

[20] Bennett MD, Leo DJ. Ionic liquids as novel solvents for ionic polymer transducers. In: EAP actuators and devices, vol. 5385. SPIE; 2004. p. 210–20.

[21] Bonhôte P, Paula Dias A, Papageorgiou N, Kalyanasundaram K, Grätzel M. Hydrophobic, highly conductive ambient-temperature molten salts. Inorganic Chemistry 1996;35:1168–78.

[22] Cooper EI, O'Sullivan EJ. New, stable, ambient-temperature molten salts. In: Proceedings of the eighth international symposium on molten salts. The Electrochemical Society; 1992. p. 386–96.

[23] Leo DJ, Farinholt K, Wallmersperger T. Computational models of ionic transport and electromechanical transduction in ionomeric polymer transducers. In: EAP actuators and devices, vol. 5759. SPIE; 2005. p. 170–81.

[24] Nemat-Nasser S. Micromechanics of actuation of ionic polymer–metal composites. Journal of Applied Physics 2002;92(5):2899–915.

[25] Shahinpoor M, Kim K. Ionic polymer–metal composites: III. Modeling and simulation as biomimetic sensors, actuators, transducers, and artificial muscles. Smart Materials and Structures 2004;13:1362–88.

[26] Akle BJ, Leo DJ, Hickner MA, McGrath JE. Correlation of capacitance and actuation in ionomeric polymer transducers. Journal of Materials Science 2005;40:3715–24.

[27] Millet P, Andolfatto F, Durand R. Preparation of solid polymer electrolyte composites: investigation of the ion-exchange process. Journal of Applied Electrochemistry 1995;25:227–32.

[28] Millet P, Andolfatto F, Durand R. Preparation of solid polymer electrolyte composites: investigation of the precipitation process. Journal of Applied Electrochemistry 1995;25:233–9.

[29] Rashid T, Shahinpoor M. Force optimization of ionic polymeric platinum composite artificial muscles by means of orthogonal array manufacturing method. In: EAP actuators and devices, vol. 3669. SPIE; 1999. p. 289–98.

[30] Akle BJ, Bennett MD, Leo DJ. High-strain ionomeric-ionic liquid electroactive actuators. Sensors and Actuators A: Physical 2005;126:173–81.

[31] Sheth JP, Unal S, Yilgor E, Yilgor I, Beyer FL, Long TE, et al. A comparative study of the structure–property behavior of highly branched segmented poly(urethane urea) copolymers and their linear analogs. Polymer 2005;46:10180–90.

[32] Bar-Cohen Y, Leary S. Electro-active polymer (EAP) characterization methods. In: EAP actuators and devices, vol. 3987. SPIE; 2000. p. 12–6.

[33] Newbury K. Characterization, modeling, and control of ionic polymer transducers. Ph.D. thesis, Virginia Tech; 2002.

[34] Gierke T. Ionic clustering in "nafion" perfluorosulfonic acid membranes and its relationship to hydroxyl rejection and chlor-alkali efficiency. In: Presented at the 152nd meeting. Atlanta, GA: The Electrochemical Society; 1977. p. 319C.

[35] Gierke T, Munn G, Wilson F. Perfluorinated ionomer membranes. American Chemical Society; 1982. p. 195–216 [chapter 10].

[36] Hashimoto T, Fujimura M, Kawai H. Perfluorinated ionomer membranes. American Chemical Society; 1982. p. 217–48 [chapter 11].

[37] Yeager HL, Steck A. Cation and water diffusion in nafion ion exchange membranes: influence of polymer structure. Journal of the Electrochemical Society 1981;128:1880–4.

[38] James P, Elliott J, McMaster T, Newton J, Elliott A, Hanna S, et al. Hydration of nafion studied by AFM and X-ray scattering. Journal of Materials Science 2000;35:5111–9.

[39] Elliott J, Hanna S, Elliott A, Cooley G. Interpretation of the small angle X-ray scattering from swollen and oriented perfluorinated ionomer membranes. Macromolecules 2000;33:4161–71.

[40] Gebel G, Lambard J. Small-angle scattering study of water-swollen perfluorinated ionomer membranes. Macromolecules 1997;30:7914–20.

[41] Mauritz KA, Moore RE. State of understanding of nafion. Chemical Reviews 2004;104:4535–85.

[42] Bennett M. Electromechanical transduction in ionic liquid-swollen nafion membranes. Ph.D. thesis, Virginia Tech; 2005.

[43] Bennett M, Leo D. Morphological and electromechanical characterization of ionic liquid/nafion polymer composites. In: EAP actuators and devices, vol. 5759. SPIE; 2005. p. 506–17.

[44] Falk M. Perfluorinated ionomer membranes. American Chemical Society; 1982. p. 139–70 [chapter 8].

[45] Heitner-Wirguin C. Infra-red spectra of perfluorinated cation-exchanged membranes. Polymer 1979;20:371–4.

[46] Lowry S, Mauritz K. An investigation of ionic hydration effects in perfluorosulfonate ionomers by Fourier transform infrared spectroscopy. Journal of the American Chemical Society 1980;102:4665–7.

[47] Shannon R. Revised effective ionic radii and systematic studies of interatomic distances in halides and chalcogenides. Acta Crystallographica 1976;A32:751–67.

[48] Koch V, Nanjundiah C, Carlin R. Hydrophobic ionic liquids. U.S. Patent 5,827,602; 1998.

[49] Sun Y-M, Favre I, Schild L, Moczydlowski E. On the structural basis for size-selective permeation of organic cations through the voltage-gated sodium channel. Journal of General Physiology 1997;110:693–715.

[50] Komoroski R, Mauritz K. Perfluorinated ionomer membranes. American Chemical Society; 1982. p. 113–38 [chapter 7].

[51] Komoroski R, Mauritz K. A sodium-23 nuclear magnetic resonance study of ionic mobility and contact ion pairing in a perfluorosulfonate ionomer. Journal of the American Chemical Society 1978;100:7487–9.

[52] Kidd RG. NMR of newly accessible nuclei, vol. 1. Academic Press; 1983. p. 103–31 [chapter 5].

[53] Zawodzinski TA, Neeman M, Sillerud L, Cottesfeld S. Determination of water diffusion coefficients in perfluorosulfonate ionomeric membranes. Journal of Physical Chemistry 1991;95:6040–4.

[54] Gebel G, Aldebert P, Pineri M. Swelling study of perfluorosulphonated ionomer membranes. Polymer 1993;34:333–9.

[55] Mueller JM. Complex impedance studies of electrosprayed and extruded nafion membranes. Trident Scholar project report, US Naval Academy, report no. 324; 2004.

[56] Rollet A-L, Diat O, Gebel G. Transport anisotropy of ions in sulfonated polyimide ionomer membranes. Journal of Physical Chemistry B 2004;108:1130–6.